

# Multiple SecA Molecules Drive Protein Translocation across a Single Translocon with SecG Inversion<sup>\*[5]</sup>

Received for publication, September 7, 2011, and in revised form, November 8, 2011. Published, JBC Papers in Press, November 10, 2011, DOI 10.1074/jbc.M111.301754

Kazuhiro Morita, Hajime Tokuda<sup>1</sup>, and Ken-ichi Nishiyama<sup>2</sup>

From the Institute of Molecular and Cellular Biosciences, The University of Tokyo, Tokyo 113-0032, Japan

**Background:** Preproteins are translocated across membranes by SecA ATPase through SecYEG with dynamic structure changes, including SecG inversion.

**Results:** A SecA mutant, together with wild-type SecA, caused SecG inversion with accumulation of translocation intermediates.

**Conclusion:** Multiple SecA molecules drive protein translocation across a translocon with SecG inversion.

**Significance:** A revised model is proposed in which a single SecA cycle causes translocation of 10–13 kDa.

SecA is a translocation ATPase that drives protein translocation. D209N SecA, a dominant-negative mutant, binds ATP but is unable to hydrolyze it. This mutant was inactive to proOmpA translocation. However, it generated a translocation intermediate of 18 kDa. Further addition of wild-type SecA caused its translocation into either mature OmpA or another intermediate of 28 kDa that can be translocated into mature by a proton motive force. The addition of excess D209N SecA during translocation caused a topology inversion of SecG. Moreover, an intermediate of SecG inversion was identified when wild-type and D209N SecA were used in the same amounts. These results indicate that multiple SecA molecules drive translocation across a single translocon with SecG inversion. Here, we propose a revised model of proOmpA translocation in which a single catalytic cycle of SecA causes translocation of 10–13 kDa with ATP binding and hydrolysis, and SecG inversion is required when the next SecA cycle begins with additional ATP hydrolysis.

Translocation of presecretory proteins across the cytoplasmic (inner) membrane of *Escherichia coli* is catalyzed mainly by SecA, a translocation ATPase, and SecYEG, a protein-conducting channel in membranes. Most presecretory proteins are synthesized as precursors with an N-terminally attached signal sequence and are translocated at least partly posttranslationally in *E. coli*. Both the SecA and SecYEG structures have been revealed by several crystal structures, facilitating the understanding of protein translocation (for reviews, see Refs. 1–4).

SecA is a translocation ATPase that is activated by presecretory proteins and IMV,<sup>3</sup> and that provides a direct driving force

for translocation through ATP binding and hydrolysis. SecA possesses several domains (see Fig. 1A), including two nucleotide binding domains (NBDs) and a precursor binding domain. SecA also has many ligands, not only ATP/ADP, precursors, SecB, and SecYEG, but also membrane lipids and SecDF, indicating that SecA undergoes numerous structure changes during the catalytic cycle of translocation (for reviews, see Ref. 3). SecA is localized both in the cytosol and on the cytoplasmic membrane (5). SecA interacts with SecYEG with high affinity, although it interacts with membrane lipids with low affinity (6). Acidic phospholipids are essential for the SecA function (6, 7). Membrane-bound SecA consists of peripherally bound and deeply integrated forms (5, 8, 9). Cytoplasmic SecA mainly forms a homodimer (10). However, several kinds of SecA dimer have been reported (3), indicative of the dynamic structure changes of SecA.

SecG is a subunit of the SecYEG translocon (11, 12) and possesses two transmembrane stretches. The membrane topology of SecG has been determined to be one with the N and C termini being exposed to the periplasmic space in the absence of translocation (Refs. 13 and 14 and Fig. 2A). On the other hand, its topology obviously changes during the translocation reaction in SecA- and preprotein-dependent manners (13). We have demonstrated that SecG undergoes a topology inversion cycle coupled with the SecA cycle (15–17), although a report has also been found in which the topology inversion model was challenged (18).

A detailed analysis of protein translocation mechanisms has been performed, especially ones using proOmpA (the precursor of outer membrane protein A) as a substrate. Identification of the translocation intermediates provided important hints for understanding the molecular mechanisms underlying translocation. Of these, ones of 16 kDa and 26 kDa (referred to as I<sub>16</sub> and I<sub>26</sub>, respectively) are likely to reflect the catalytic cycle of SecA because they are stably generated at low ATP concentrations (19, 20). The findings that these intermediates are further translocated by approximately 2 kDa on the addition of a non-hydrolyzable analog of ATP (19, 20) or sodium azide (21) and

\* This work was supported by grants-in-aid for scientific research from the Ministry of Education, Culture, Sports, Science, and Technology of Japan.

[5] This article contains supplemental Fig. 1.

<sup>1</sup> Present address: Faculty of Nutritional Sciences, University of Morioka, Takizawa, Iwate 020-0183, Japan.

<sup>2</sup> To whom correspondence should be addressed: Cryobiofrontier Research Center, Faculty of Agriculture, Iwate University, Morioka, Iwate 020-8550, Japan. Tel.: 81-19-621-6471; Fax: 81-19-621-6243; E-mail: nishiyam@iwate-u.ac.jp.

<sup>3</sup> The abbreviations used are: IMV, inverted membrane vesicle(s); NBD, nucleotide binding domain; proOmpA, precursor of outer membrane protein A;

PMF, proton motive force; AMP-PNP, adenylylimidodiphosphate; m, mature OmpA.

## SecA-SecG Cycle in Preprotein Translocation

that such an analog itself causes processing of the signal sequence (20) reveal that ATP binding to SecA results in translocation of proOmpA by 2–3 kDa. Membrane insertion of radiolabeled SecA was found to be proOmpA translocation-dependent (22, 23), supporting the idea of stepwise translocation coupled with an “insertion-deinsertion cycle of SecA.” On the other hand, the crystal structure of the SecYEG-SecA complex suggested that SecA is localized rather far from the membrane surface (24). Furthermore, the size of the SecYEG pore determined with an archaea translocon seems too small for the membrane insertion of both SecA and proOmpA (25). These findings are unfavorable for the SecA insertion model. Moreover, no translocation intermediates other than  $I_{16}$ ,  $I_{26}$ , and derivatives of them have been identified so far. Nonetheless, an inverted topology of SecG is fixed through inhibition of ATP hydrolysis during proOmpA translocation, and the original topology is then recovered on ATP hydrolysis or removal of membrane-associated SecA (13). However, to detect SecG inversion, soluble SecA is essential (17). Therefore, a single SecA cycle cannot be explained by a simple SecA insertion-deinsertion model.

To clarify the catalytic cycle of SecA and the relationship between the SecA and SecG cycles, we employed dominant-negative mutants of SecA in which ATP hydrolysis was impaired. D209N SecA possesses a mutation in Walker motif B in NBD 1 and R509K SecA one in Walker motif A in NBD 2 (26). D209N SecA binds ATP but is unable to hydrolyze it (23). We found that D209N SecA generated a translocation intermediate of proOmpA that can be translocated into mature by wild-type SecA and proton motive force (PMF), indicating that multiple SecA molecules function on a single translocon. D209N SecA, together with wild-type SecA, not only caused topology inversion of SecG but also allowed the identification of an intermediate of SecG inversion. We also propose a revised model of the SecA cycle with SecG inversion.

### EXPERIMENTAL PROCEDURES

**Materials**—IMV were prepared from K003 (HfrH *pnp-13 tyr met RNaseI<sup>-</sup> Lpp<sup>-</sup> ΔuncB-C::Tn10* (27) or its *secG* deficient strain, KN553 (28), as described (29). WT SecA (30) and SecB (16) were purified from SecA and SecB overproducers, respectively, as described. Anti-SecG antibodies were raised in a rabbit using a synthetic peptide corresponding to the C-terminal 16 amino acids of SecG (11). SecA was labeled with  $\text{Na}^{125}\text{I}$  (629 GBq/mg I, MP Biochemicals) by means of Iodogen (Pierce) as described previously (15). The specific activity was  $\sim 4 \times 10^6$  cpm/ $\mu\text{g}$  SecA. ProOmpA was prepared from an OmpA-overproducing strain as described previously (31).  $^{35}\text{S}$ -Labeled proOmpA was synthesized *in vitro* in the presence of a  $\text{Tran}^{35}\text{S}$ -label, a mixture of [ $^{35}\text{S}$ ]Met and [ $^{35}\text{S}$ ]Cys (MP Biochemicals), using plasmid pSI053 as a template (29). ATP, AMP-PNP, creatine kinase, and creatine phosphate were purchased from Roche. Contamination by ATP in AMP-PNP was <0.1%. NADH, succinate, pyruvate kinase, and lactate dehydrogenase were from Sigma. Proteinase K was from Merck.

**Purification of Mutant SecAs**—D209N SecA and R509K SecA were purified from BL21.19 (BL21 (ADE3) *secA13(am) supF(ts) trp(am) zch::Tn10 recA::cat clpA::kan*) harboring plasmids

pD209N and pR509K, respectively (26). After these cells had been cultivated in Luria-Bertani (LB) medium at 30 °C to  $\sim 5 \times 10^8$  cells/ml, an equal volume of LB medium, which had been preheated at 52 °C, was mixed to stop the expression of wild-type *secA*, followed by the induction of the mutant SecAs by the addition of 0.1 mM isopropyl 1-thio- $\beta$ -D-galactopyranoside. After allowing the expression of the mutant SecAs at 41 °C for 1 h, cells were harvested. Because both mutant SecAs were recovered mostly in the IMV fraction, IMV (10 mg/ml) were extracted with 5 M urea and 50 mM potassium phosphate (pH 7.5) for 1 h on ice, followed by centrifugation at  $150,000 \times g$  for 2 h at 4 °C. The resultant supernatants were dialyzed against 50 mM potassium phosphate (pH 7.5) and 1 mM dithiothreitol to remove urea and to allow refolding of the SecAs as described (32). The mutant SecAs were then purified as described for WT SecA (30). The N termini of the purified preparations were confirmed by means of an Applied Biosciences Protein Sequencer 477A.

**Translocation of proOmpA**—The translocation reaction mixture was composed of IMV (200  $\mu\text{g}/\text{ml}$  as IMV protein), SecB (50  $\mu\text{g}/\text{ml}$ ), ATP (1 mM), and an ATP regenerating system (5 mM creatine phosphate and 10  $\mu\text{g}/\text{ml}$  creatine kinase) in 50 mM potassium phosphate (pH 7.5), 1 mM  $\text{MgSO}_4$ , and 2 mM DTT. SecA and proOmpA were added as specified. The reaction was initiated by adding proOmpA ( $\sim 5000$  cpm/ $\mu\text{l}$ ) at 37 °C. The cold proOmpA (25  $\mu\text{g}/\text{ml}$ ) was premixed as specified. At each indicated time, an aliquot (25  $\mu\text{l}$ ) was withdrawn and treated with proteinase K (1 mg/ml) on ice for 30 min. The translocated materials should be protected by membranes from the proteinase K digestion. They were then analyzed by SDS-PAGE and autoradiography, followed by determination using an ATTO densitograph.

**SecG Inversion assay**—The translocation reaction was carried out as described above except that only cold proOmpA (25  $\mu\text{g}/\text{ml}$ ) was used. After the reaction had been allowed to proceed at 37 °C for 5 min, 20 mM AMP-PNP and 20 mM  $\text{MgSO}_4$  were added. AMP-PNP was prepared immediately prior to the reaction. The mutant SecA was added instead of AMP-PNP as specified. After further incubation at 37 °C for 5 min, the reaction mixture was chilled on ice, followed by proteinase K digestion. SecG and its C-terminal 9 kDa fragment were detected on immunoblotting as described (13).

**SecA Insertion/Deinsertion Assay**—The translocation reaction was carried out using IMV washed with 4 M urea (28) and cold proOmpA (25  $\mu\text{g}/\text{ml}$ ).  $^{125}\text{I}$ -Labeled SecA (0.4  $\mu\text{g}/\text{ml}$ ) was added to start the reaction at 37 °C. Where specified, non-labeled SecA was added. At each indicated time, an aliquot (100  $\mu\text{l}$ ) was withdrawn and digested with 1 mg/ml proteinase K. The membrane-protected 30-kDa fragment was analyzed by SDS-PAGE and then by autoradiography, followed by quantification by means of an ATTO densitograph.

**Other Methods**—To analyze OmpA and SecA, an SDS gel was used as described (33), whereas the analysis of SecG was performed as described previously (34). Immunoblotting was carried out as described (35). Translocation ATPase activity was determined by means of an enzyme-coupled method as described (36). Protein was determined as described (37) using BSA as a standard.

## RESULTS

**Effect of Dominant Negative SecA Mutants on proOmpA Translocation**—It is thought that dominant negative SecA mutants form a dead-end complex with the translocon causing cell death (23, 26). Consistent with this idea, the majority of overproduced D209N SecA (>90%, Fig. 1B) and R509K SecA (>80%, data not shown) was recovered with membranes. To confirm the dominant negative effect of D209N and R509K SecA on proOmpA translocation, purified D209N SecA and R509K SecA mutants were added to monitor proOmpA translocation into IMV prepared from K003 cells (*sec*<sup>+</sup>  $\Delta$ *unc*). PMF was not imposed to examine the SecA function precisely. In the absence of externally added SecA, where translocation is driven by membrane-bound SecA, only low proOmpA translocation activity was observed (Fig. 1, C and D, *no addition*). The addition of wild-type SecA (WT SecA) caused significant stimulation of proOmpA translocation (+*wt SecA*), as reported previously (17, 38). When D209N SecA or R509K SecA was added instead of WT SecA, proOmpA translocation was completely abolished (+*D209N SecA* and +*R509K SecA*, respectively), indicating that these SecA mutants were dominant over membrane-bound WT SecA. The dominant negative feature of these mutants was also confirmed by analyzing translocation ATPase activity, which is induced by IMV and proOmpA (Fig. 1E). Translocation ATPase activity obtained with a fixed amount of WT SecA (10  $\mu$ g/ml) decreased as the amounts of the mutants increased. The inhibitory effect of D209N SecA was significantly higher than that of R509K SecA. The ATPase activity was not completely abolished even when the mutants were added in excess over WT SecA, however.

**D209N SecA Induces Topology Changes of SecG Together with WT SecA**—An inverted topology of SecG can be fixed under certain conditions (13, 39). Because SecG inversion is controlled by the ATPase activity of SecA, we examined the effects of the SecA mutants on SecG inversion. SecG possesses two transmembrane stretches with the N- and C termini being exposed to periplasm (Refs. 13 and 14 and Fig. 2A, *left panel*). When IMV were digested with proteinase K, a 9-kDa fragment could be detected on immunoblots using anti-SecG antibodies that recognize the C terminus (Ref. 13 and Fig. 2B, *-ATP*). When the topology of SecG was inverted, the antigenic region is digested by proteinase K, giving neither intact SecG nor a 9-kDa fragment (Ref. 13 and Fig. 2A, *center panel*). When a non-hydrolyzable analog of ATP, adenylylimidodiphosphate (AMP-PNP), was added during proOmpA translocation, externally added proteinase K digested the C-terminal region of SecG without giving rise to the 9-kDa fragment, indicating that the inverted topology of SecG was fixed (Fig. 2B, *complete*  $\rightarrow$  *AMP-PNP*). A high concentration of AMP-PNP (20 mM) was necessary, because affinity of AMP-PNP to SecA is much lower than that of ATP or ADP (40). When D209N SecA was added during proOmpA translocation in an excess amount (20  $\mu$ g/ml) over WT SecA (2  $\mu$ g/ml), SecG was efficiently inverted even in the absence of AMP-PNP (Fig. 2B, *complete*  $\rightarrow$  +*D209N SecA*). When ATP (*-ATP*  $\rightarrow$  +*AMP-PNP*) or SecA (*-SecA*  $\rightarrow$  +*AMP-PNP*) was omitted, SecG inversion was not observed as in the complete translocation reaction (*complete*), indicating that fix-

ation of inverted SecG by AMP-PNP is translocation-dependent. The AMP-PNP-like effects of D209N SecA are consistent with the mutant characteristics that D209N SecA binds to ATP but is unable to hydrolyze ATP (23). On the other hand, SecG inversion was not observed on the addition of R509K SecA (data not shown). Hereafter, we focused on the effects of D209N SecA.

The effects of D209N SecA on SecG inversion were further characterized. When proOmpA translocation was carried out with WT SecA (120  $\mu$ g/ml), the 9-kDa fragment was generated upon proteinase K digestion, albeit at a reduced level (Fig. 2C, *wt SecA*). SecG inversion was again observed on the addition of AMP-PNP during translocation (*wt SecA*  $\rightarrow$  *AMP-PNP*). When only D209N SecA (120  $\mu$ g/ml) was used, essentially no SecG inversion was observed, giving rise to the 9-kDa fragment (*D209N SecA*). On the other hand, when both WT SecA and D209N SecA were added in the same amounts (60  $\mu$ g/ml each), the 9-kDa fragment was not generated at all (*D209N SecA* + *wt SecA*). Although the amount of intact SecG clearly decreased, which was indicative of SecG inversion, nearly half of SecG was resistant to proteinase K digestion (lanes at 100 and 1000  $\mu$ g/ml). This SecG topology does not fit with either the original (Fig. 2A, *left panel*) or the inverted (*center panel*) one. Instead, this seems to be a novel intermediate state depicted on the right, which externally added proteinase K could not access. The generation of this intermediate of SecG was also observed when proOmpA translocation was initiated using WT SecA, followed by the addition of the same amount of D209N SecA (*wt SecA*  $\rightarrow$  *D209N SecA*). Even when the order of addition of WT SecA and D209N SecA was reversed, a similar result was obtained (*D209N SecA*  $\rightarrow$  *wt SecA*). In this case, a small amount of the 9-kDa fragment was also detected. These results indicate that D209N SecA affects the SecG topology together with WT SecA, giving inverted and intermediate topologies of SecG. These results were not caused by adding SecA twice during reactions because the 9-kDa fragment was observed when the same kind of SecA was added during reactions (*wt SecA*  $\rightarrow$  +*wt SecA* and *D209N SecA*  $\rightarrow$  +*D209N SecA*).

Because both the SecA and SecG cycles are driven by ATP, we next examined the effect of a low concentration of ATP (Fig. 2D). When ATP was omitted from the translocation reaction (*-ATP*) or when translocation was carried out in the presence of 1 mM ATP (+1 mM ATP), the 9-kDa band was clearly generated, whereas SecG was completely inverted when AMP-PNP was added during translocation (1 mM ATP  $\rightarrow$  *AMP-PNP*). On the other hand, when the ATP concentration was reduced to 10  $\mu$ M, the amount of the 9-kDa fragment was reduced by half with loss of the SecG band (+10  $\mu$ M ATP), indicating that half of SecG was inverted under the conditions, without the intermediate topology generated by D209N SecA. It is known that some translocation intermediates of proOmpA can be formed under these conditions (20).

**D209N SecA Causes the Accumulation of Translocation Intermediates of proOmpA**—To determine whether or not D209N SecA also affects the generation of intermediates of proOmpA translocation, we next chased each translocation process in detail using radiolabeled proOmpA to follow a single-round reaction. Several kinds of translocation intermedi-

## SecA-SecG Cycle in Preprotein Translocation

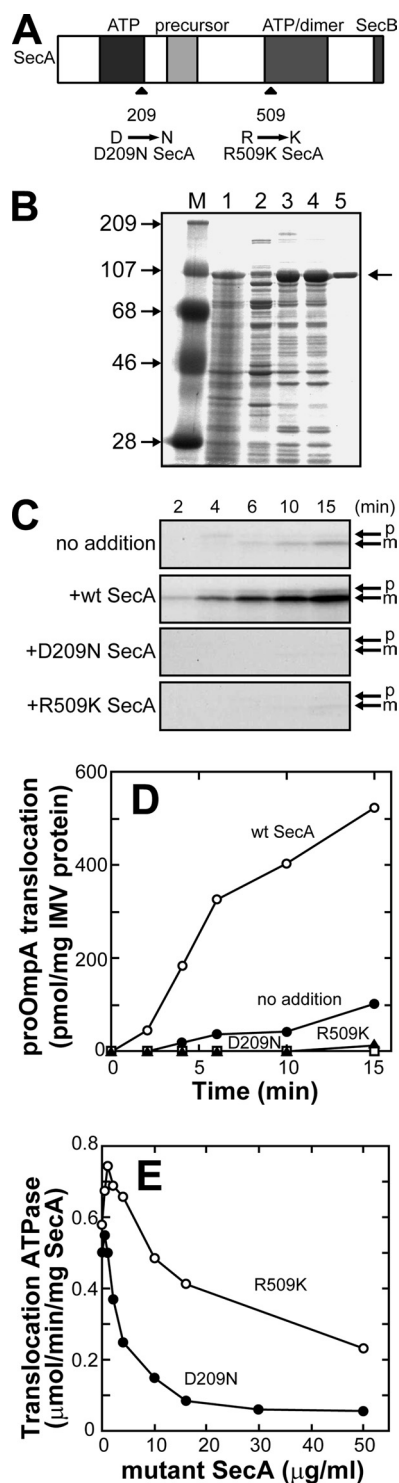


**FIGURE 1. Purification of the SecA mutants and their effects on proOmpA translocation.** *A*, schematic representation of SecA and the mutation points. Domains interacting with specific ligands are indicated. *B*, purification of D209N SecA. Molecular markers (lane *M*), sizes in kDa at left, a total cell lysate (lane 1), cytosol (lane 2), IMV (lane 3), a urea extract (lane 4), and the purified preparation (lane 5) were analyzed by SDS-PAGE and Coomassie Brilliant Blue staining. 20  $\mu\text{g}$  of each fraction or 2  $\mu\text{g}$  of purified preparation was applied on gel. *C*, the translocation reaction was carried out in the presence or absence (no addition) of the indicated SecA (60  $\mu\text{g}/\text{ml}$ ), using IMV prepared from K003 and proOmpA (25  $\mu\text{g}/\text{ml}$ ) as a substrate. The translocated proOmpA (*p*) and OmpA (*m*) are indicated. *D*, the translocated materials shown in *C* were quantitated and plotted against time. The numbers of Met and Cys of 8 and 7 in *p* and *m*, respectively, were used for calculations. *E*, the effects of the mutant SecAs on the translocation ATPase activity. The translocation reaction was

carried out in the presence of a fixed amount of WT SecA (10  $\mu\text{g}/\text{ml}$ ) and the indicated amounts of a mutant SecA. The increase in ATPase activity on the addition of proOmpA (25  $\mu\text{g}/\text{ml}$ ) was measured and plotted against the concentration of mutant SecA.

ates of proOmpA have been reported (19, 20, 31), *i.e.*  $I_{16}$ ,  $I_{18}$ ,  $I_{26}$ ,  $I_{28}$ , and  $I_{29}$ , named after their molecular weights. Of these,  $I_{16}$  and  $I_{26}$  are generated as a result of the SecA cycle because they can be stably detected when proOmpA translocation is carried out in the presence of a low ATP concentration (20).  $I_{18}$  and  $I_{28}$  are derivatives of  $I_{16}$  and  $I_{26}$ , generated through a single SecA insertion upon ATP binding because AMP-PNP addition transforms  $I_{16}$  and  $I_{26}$  into  $I_{18}$  and  $I_{28}$ , respectively (19, 20). On the other hand,  $I_{29}$  is an intermediate whose translocation is stopped by the artificial formation of an intramolecular disulfide bridge (31). When WT SecA was used for proOmpA translocation, not only fully translocated and processed mature OmpA (*m*) of 34 kDa but also some intermediates, including  $I_{26}$  and  $I_{29}$ , were observed (Fig. 3*A*, *wt SecA*).  $I_{26}$  appeared transiently only at the initial stage of the reaction, confirming that this intermediate is formed prior to the completion of translocation (19). On the other hand,  $I_{29}$  marginally appeared because of the non-oxidizing conditions, as reported (31). In marked contrast, when D209N SecA was used for proOmpA translocation,  $I_{18}$  was specifically detected, indicating that even the mutant SecA translocated up to this form of proOmpA (D209N SecA). Further addition of WT SecA to the reaction caused the generation of  $I_{28}$  and *m* in addition to a small amount of  $I_{26}$  ( $\rightarrow$  *wt SecA*).  $I_{28}$  and *m* increased with similar kinetics, whereas  $I_{26}$  and  $I_{18}$  decreased. Therefore,  $I_{28}$  seems to be a dead-end product that cannot be translocated into *m*. When WT SecA and D209N SecA were added at the same time, essentially a similar result was obtained (*wt SecA* + D209N SecA). These results strongly suggest that WT SecA translocated  $I_{18}$  into  $I_{26}$  and then into either  $I_{28}$  or *m*. They also indicate that WT SecA functions on IMV carrying D209N SecA in a saturated amount. Determination of the translocated amounts at 10 min, when the reaction had reached plateau level, revealed that the sum of  $I_{18}$ ,  $I_{28}$ , and *m* is almost the same under WT SecA and D209N SecA/WT SecA conditions, whereas it was less in D209N SecA (Fig. 3*B*). Also, it was found that the amounts of  $I_{28}$  and *m* were the same when both WT SecA and D209N SecA were present, supporting the idea that  $I_{18}$  is converted into either  $I_{28}$  or *m*.

The results in Figs. 2 and 3*A* indicate that D209N SecA can affect the translocon together with WT SecA. On the other hand, it has been reported that D209N SecA is unable to deinsert to form a dead-end complex (23). The formation of  $I_{28}$  or completion of translocation (Fig. 3*A*) after  $I_{18}$  formation suggests that WT SecA can act on the D209N SecA-translocon complex. Therefore, we next examined whether or not radiolabeled SecA was inserted into D209N SecA-loaded IMV in which  $I_{18}$  had been accumulated (Fig. 3*C*).  $^{125}\text{I}$  D209N SecA insertion into D209N SecA/proOmpA-loaded IMV was not observed, indicating that all the translocon had been occupied by D209N SecA/proOmpA under these conditions. On the other hand,  $^{125}\text{I}$  WT SecA insertion into such IMV could be observed as a proteinase K-protected band corresponding to 30 kDa. Although the level of the inserted SecA was low, it was

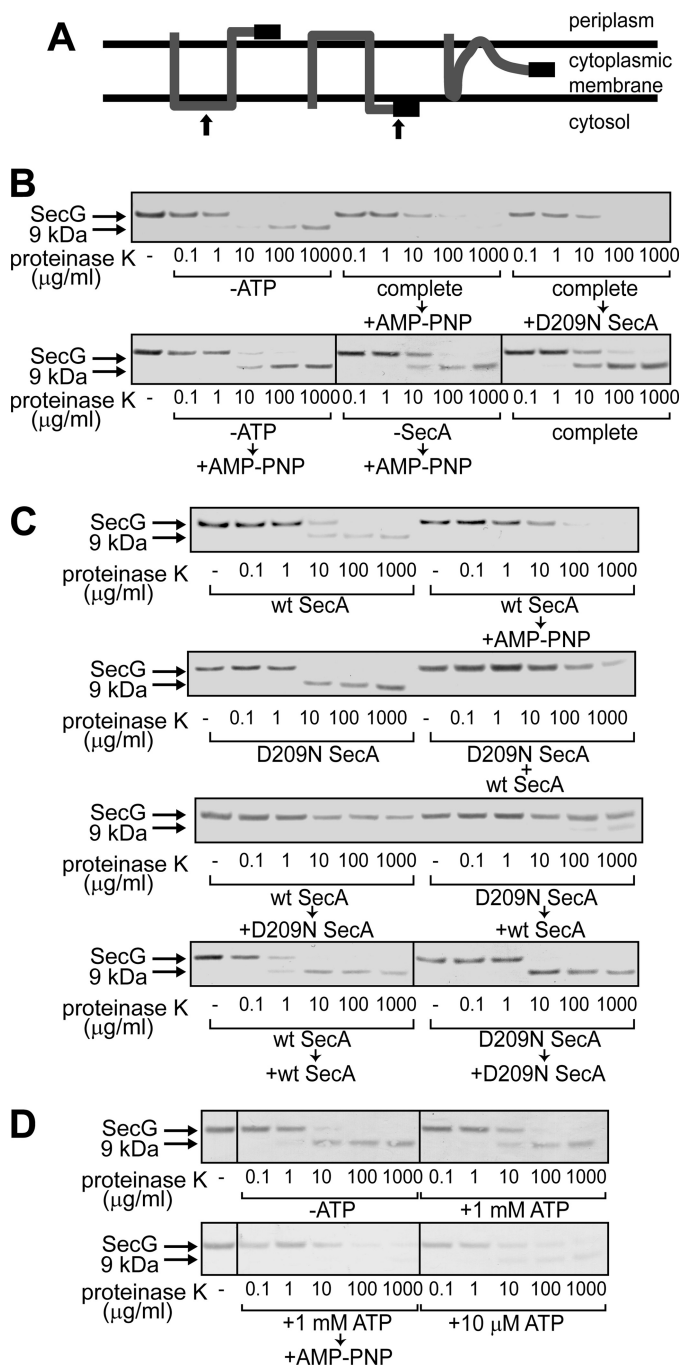


**FIGURE 2. Topology changes of SecG induced by D209N SecA.** *A*, topology arrangement of SecG. SecG possesses two transmembrane stretches with its N and C termini being exposed to the periplasmic space (left). When inverted, both termini are exposed to the cytoplasmic side (center). At the right, the intermediate topology is shown. The black bar represents the antigenic region of the anti-SecG antiserum. The arrows at the left and center indicate the positions where proteinase K added outside of IMV cleaves SecG. *B*, addition of an excess amount of D209N SecA during proOmpA translocation caused SecG inversion. ProOmpA translocation into IMV prepared from K003 was carried out in the presence of 2 μg/ml WT SecA, as described under "Experimental Procedures" (complete). Where specified, ATP and SecA were omitted (-ATP and -SecA, respectively). At 5 min after initiation of the translocation reaction, either 20 mM AMP-PNP/MgSO<sub>4</sub> (+AMP-PNP) or 20 μg/ml D209N SecA (+D209N SecA) was added as specified. After the reaction mixtures had been incubated for further 5 min, they were chilled on ice, followed by proteinase K digestion at the indicated concentrations. Samples were then analyzed by SDS-PAGE and immunoblotting using anti-SecG antiserum. The bands of SecG and the C-terminal 9 kDa are indicated by arrows. *C*, D209N SecA together with WT SecA causes the intermediate topology of SecG. The

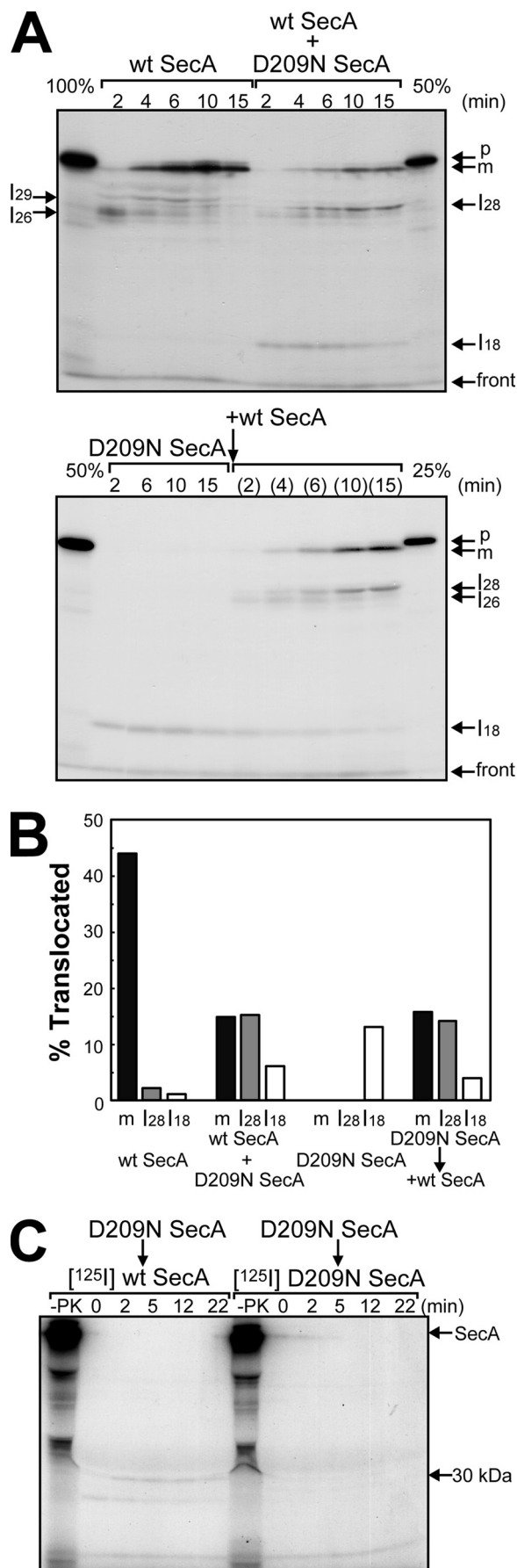
specific for WT SecA. These results indicate that WT SecA can act even on the D209N SecA-translocon complex.

Next, we examined whether or not I<sub>28</sub>, which seemed to be a dead-end product formed by D209N SecA, can be converted into m by PMF (Fig. 4). After I<sub>18</sub> had been formed by D209N SecA, WT SecA was added. As shown in Fig. 3A, I<sub>26</sub> transiently, and then I<sub>28</sub> and m, were observed with a decrease in I<sub>18</sub>. When PMF was imposed at 20 min, m increased with a decrease in I<sub>28</sub>, indicating that PMF translocated I<sub>28</sub> into m. We also treated samples at 15 and 20 min with urea prior to proteinase K digestion. Such urea treatment removes the membrane-bound SecA and thereby causes the recovery of the original topology of SecG (13). With this treatment, approximately half of mature OmpA and all the I<sub>28</sub> disappeared, a new band corresponding to ~24 kDa (asterisk) being generated (Fig. 4A, 15\* and 20\*). These results indicate that a part of the translocated materials was backward-translocated into the 24-kDa material. Moreover, it is likely that I<sub>28</sub> and half of the mature OmpA were still bound to SecA. Because I<sub>26</sub> is backward-translocated even into I<sub>16</sub> on urea treatment (20), I<sub>28</sub> should be a one-step-later intermediate than I<sub>26</sub> in the SecA cycle.

*SecG Stabilizes Membrane-associated SecA*—To clarify the relationship between SecA insertion and the SecG function in more detail, SecA insertion into ΔSecG IMV was examined (Fig. 5 and supplemental Fig. 1). When <sup>125</sup>I WT SecA was used to monitor SecA insertion, efficient SecA insertion into SecG<sup>+</sup> IMV was observed, whereas that into ΔSecG IMV was reduced. In both cases, the inserted SecA was replaced and deinserted on the addition of an excess amount of cold SecA (Fig. 5A), as reported previously (15, 22). When <sup>125</sup>I D209N SecA was used, similar levels of SecA insertion into both types of IMV were observed, confirming the normal insertion ability of the mutant SecA. The SecA inserted into SecG<sup>+</sup> IMV was not deinserted and replaced on the addition of cold SecA because deinsertion/replacement requires ATP hydrolysis (22). On the other hand, when cold SecA was added to ΔSecG IMV to which <sup>125</sup>I D209N SecA had been inserted, a decrease in the inserted SecA was observed (Fig. 5B), indicating that the deinsertion-deficient mutant SecA can be deinserted if SecG is missing. This effect was examined more precisely using various amounts of cold SecA (Fig. 5C). When SecG<sup>+</sup> IMV were used, D209N SecA deinsertion was not observed at any concentration. In contrast, the level of the SecA inserted into ΔSecG IMV decreased as the concentration of cold SecA increased, confirming that the mutant SecA can be deinserted and replaced on ΔSecG IMV.

translocation reaction was initiated in the presence of WT SecA (wt SecA, wt SecA → AMP-PNP, wt SecA → D209N SecA, wt SecA → wt SecA), D209N SecA (D209N SecA, D209N SecA → wt SecA, D209N SecA → D209N SecA), or both (D209N SecA + wt SecA). The samples indicated by arrows received the indicated materials (20 mM AMP-PNP/MgSO<sub>4</sub>, WT SecA, or D209N SecA) 5 min after initiation of the reactions. The SecA concentration with one kind of SecA was 120 μg/ml, whereas that with two kinds was 60 μg/ml each. After all samples had been incubated at 37 °C for 10 min in total, they were chilled on ice, followed by proteinase K digestion and SDS-PAGE/immunoblotting as in *B*. *D*, a low concentration of ATP causes a change in the SecG topology. The proOmpA translocation reaction mixtures contained 60 μg/ml WT SecA and different concentrations of ATP (0 mM -ATP, 1 mM +1 mM ATP and complete → +AMP-PNP, and 10 μM +10 μM ATP). The reaction was allowed at 37 °C for 10 min. For the "complete → +AMP-PNP" sample, 20 mM AMP-PNP/MgSO<sub>4</sub> was added at 5 min. Samples were processed as described in *B* and *C*.

## SecA-SecG Cycle in Preprotein Translocation



These results indicate that SecG stabilized the membrane-associated SecA.

## DISCUSSION

In this study, we examined the mechanism underlying proOmpA translocation using a mutant SecA in which ATP hydrolysis was impaired. D209N SecA was originally thought to bind ATP at a high affinity binding site (26) but to be unable to hydrolyze it, forming a dead-end complex with the translocon (23). We found that WT SecA can act even on the dead-end complex (Fig. 3C), causing the appearance of translocation intermediates of proOmpA (Fig. 3A) and structure changes of SecG (Fig. 2C). From these observations, we conclude that multiple SecA molecules drive protein translocation across a single translocon with SecG inversion.

Translocation intermediates of proOmpA have been characterized in several ways, including artificial cross-linking techniques (41–44) and suboptimal conditions for the reactions (20, 21, 45). Of these intermediates, I<sub>16</sub> and I<sub>26</sub> have been identified, especially when the ATP concentration is reduced in the reaction (20), strongly suggesting that they are intermediates reflecting the SecA cycle. When AMP-PNP was added to IMV carrying I<sub>16</sub> and I<sub>26</sub>, they are further translocated by as much as ~2 kDa, giving I<sub>18</sub> and I<sub>28</sub>, indicating that I<sub>18</sub> and I<sub>28</sub> are derivatives of I<sub>16</sub> and I<sub>26</sub>, respectively (19, 20). The intermediates specific for D209N SecA were the same as I<sub>18</sub> and I<sub>28</sub> in size. Because they were formed as a result of a defect in the SecA cycle, we assumed that they can be discussed on the same basis as the previously characterized intermediates. As to the catalytic cycle of SecA, a simple insertion-deinsertion model has been proposed to explain the stepwise mode of translocation (15, 22, 23, 46). AMP-PNP-dependent processing of proOmpA (20), and conversion of I<sub>16</sub> and I<sub>26</sub> into I<sub>18</sub> and I<sub>28</sub>, respectively (19, 20), are consistent with the model. However, no other intermediates have been identified so far except for I<sub>29</sub>, which is not an intermediate of the SecA cycle (31). If translocation pro-

**FIGURE 3. Translocation intermediates of proOmpA translocation.** A, [<sup>35</sup>S]proOmpA translocation into IMV prepared from K003 was carried out at 37 °C in the presence of 60 μg/ml WT SecA (upper left), D209N SecA (lower left), or both (60 μg/ml each, upper right). 15 min after the D209N SecA reaction had been initiated, WT SecA (60 μg/ml) was added and the reaction was continued at 37 °C for the periods indicated in parentheses (lower right). At each indicated time, an aliquot (25 μl) was withdrawn and chilled on ice to stop the reaction, followed by proteinase K treatment (1 mg/ml). The samples were analyzed by SDS-PAGE and autoradiography. The indicated amounts of proOmpA that had not been digested were also determined. The positions of proOmpA and mature OmpA are indicated by arrows denoted by p and m, respectively. The positions of the translocation intermediates are also indicated by arrows denoted by I<sub>29</sub>, I<sub>28</sub>, I<sub>26</sub>, and I<sub>18</sub>, respectively. B, the translocation activity of each sample in A at 10 min was quantitated. Black, gray, and white bars correspond to m, I<sub>28</sub>, and I<sub>18</sub>, respectively. The numbers of Met and Cys in OmpA, I<sub>28</sub>, and I<sub>18</sub> were regarded as 7, 4, and 4, respectively, on the basis of their molecular weights and amino acid sequences. C, [<sup>125</sup>I] WT SecA can insert into D209N SecA-saturated IMV. The translocation reaction for IMV prepared from K003 was carried out in the presence of 6 μg/ml D209N SecA and 25 μg/ml proOmpA at 37 °C for 10 min, and then either [<sup>125</sup>I] WT SecA (left) or [<sup>125</sup>I] D209N SecA (right) was added at 0.4 μg/ml, followed by further incubation at 37 °C. At each indicated time after the labeled SecA was added, an aliquot (100 μl) was withdrawn and chilled on ice, followed by proteinase K digestion at 1 mg/ml. Samples were then analyzed by SDS-PAGE and autoradiography. The sample from each reaction that had not been digested was also analyzed (-PK). The positions of SecA and the membrane-protected fragment of 30 kDa are indicated by arrows.

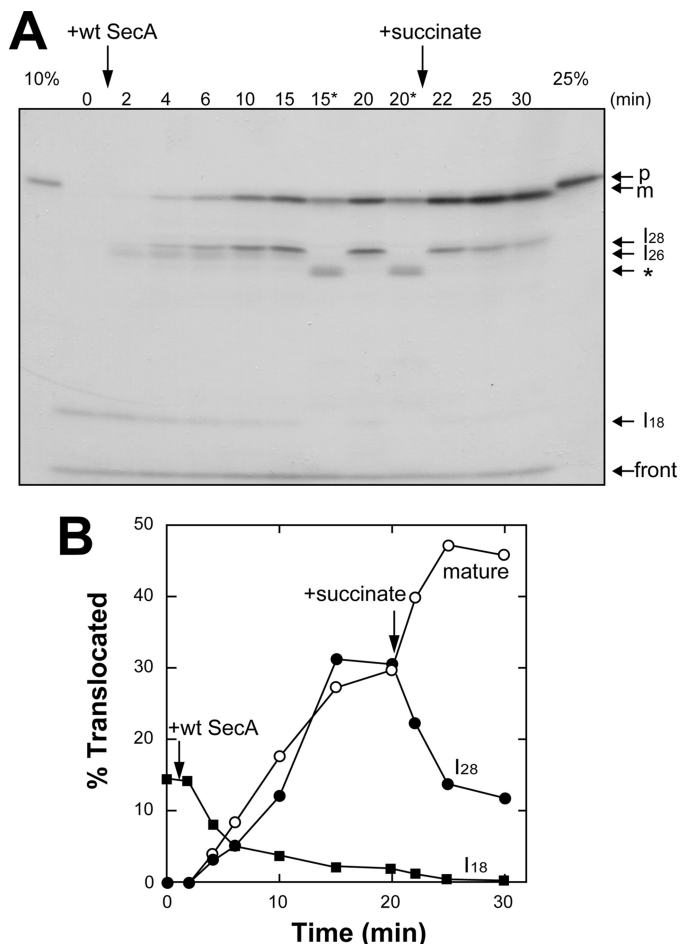


**FIGURE 4. PMF drives translocation of I<sub>28</sub> into mature OmpA.** A, [<sup>35</sup>S]proOmpA translocation was carried out in the presence of D209N SecA (60 μg/ml) as described in Fig. 3A, D209N SecA, for 15 min at 37 °C, followed by the addition of WT SecA (60 μg/ml). The time after WT SecA addition is indicated. At 20 min, PMF was imposed by adding 5 mM succinate. At each indicated time, an aliquot (25 μl) was withdrawn and chilled on ice to stop the reaction, followed by proteinase K (1 mg/ml) digestion. For the 15- and 20-min samples, the same amount (25 μl) was mixed with the same amount of a urea (8 M) solution, followed by incubation on ice for 5 min before proteinase K digestion (15' and 20', respectively). The positions of proOmpA (p) and mature OmpA (m), together with those of intermediates (I<sub>28</sub>, I<sub>26</sub> and I<sub>18</sub>) are indicated by arrows. The specific band after urea treatment (asterisk) and that at the gel front are also indicated. B, the translocated bands detected in A were quantitated and plotted against time after WT SecA addition. The numbers of Met and Cys were considered to be as in Fig. 3B.

ceeds by every 2–3 kDa, then various intermediates, as a ladder, should be identified. Alternatively, the SecA cycle might be composed of two steps, one causing a 2–3 kDa translocation with ATP binding and the other causing an 8–13 kDa translocation with ATP hydrolysis, giving only I<sub>16</sub>/I<sub>18</sub> and I<sub>26</sub>/I<sub>28</sub>. Processing of proOmpA through ATP binding, causing an ~3 kDa translocation, should be the first step of the SecA cycle, followed by translocation with ATP hydrolysis, giving I<sub>16</sub>. Considering that I<sub>18</sub> is immediately derived from I<sub>16</sub> through ATP binding, the generation of I<sub>18</sub> by D209N SecA itself suggests that this mutant undergoes a single round of the SecA cycle giving I<sub>16</sub>, and the reaction stops after next ATP binding giving I<sub>18</sub>. The fact that urea treatment of IMV carrying I<sub>26</sub> causes its backward translocation into I<sub>16</sub> (20) supports this idea.

SecG inversion could be observed on the addition of D209N SecA during proOmpA translocation. Because D209N SecA

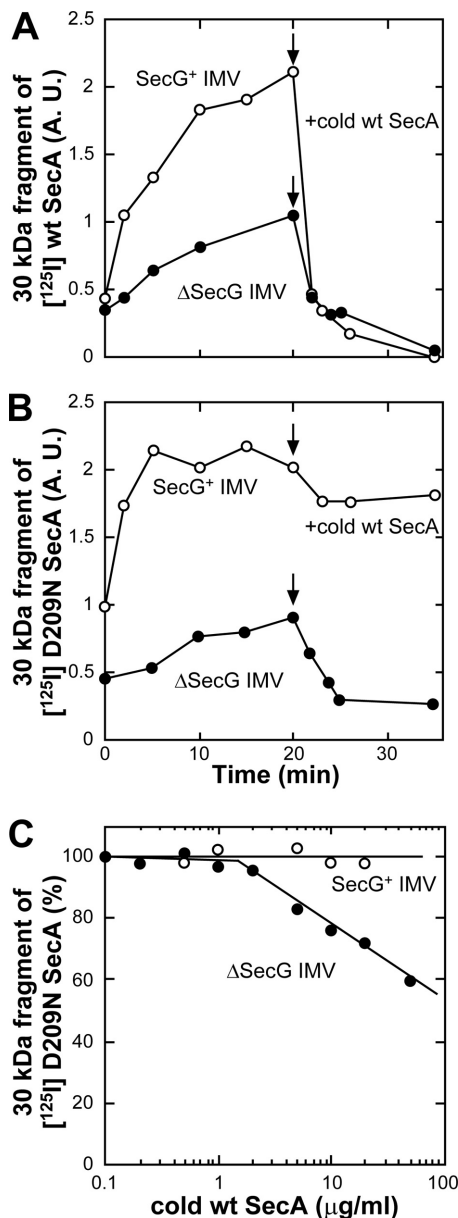


**FIGURE 5. SecG prevents dislocation of inserted SecA.** A and B, proOmpA translocation into 4 M urea-washed IMV prepared from K003 (SecG<sup>+</sup> IMV) or KN553 (ΔSecG IMV) was carried out at 37 °C using either [<sup>125</sup>I] WT SecA (A) or [<sup>125</sup>I] D209N SecA (B) as described under “Experimental Procedures.” At 20 min, cold WT SecA (60 μg/ml) was added to the reactions. An aliquot (100 μl) was withdrawn at each indicated time and chilled on ice, followed by proteinase K digestion (1 mg/ml). The membrane-protected fragment of [<sup>125</sup>I]-labeled SecA of 30 kDa was quantitated and plotted against reaction time. C, ProOmpA translocation was initiated as described in B using [<sup>125</sup>I] D209N SecA (0.4 μg/ml). At 20 min, cold WT SecA was added at the indicated concentrations, and the reaction was continued for a further 20 min. Samples were then chilled and digested with proteinase K (1 mg/ml). The membrane-protected fragment of [<sup>125</sup>I]-labeled SecA of 30 kDa was quantitated. It was expressed as a percentage of that in the respective IMV at 0.1 μg/ml and plotted against SecA concentration.

itself did not cause SecG inversion in which I<sub>18</sub> could be formed, both WT SecA and D209N SecA are involved in the fixation of the inverted SecG, consistent with our earlier observation that cytosolic SecA is essential for SecG inversion (17). As discussed above, D209N SecA is not a simple inhibitor of translocation. Therefore, an intermediate of SecG inversion could be identified in the presence of the same levels of the mutant and wild-

## SecA-SecG Cycle in Preprotein Translocation

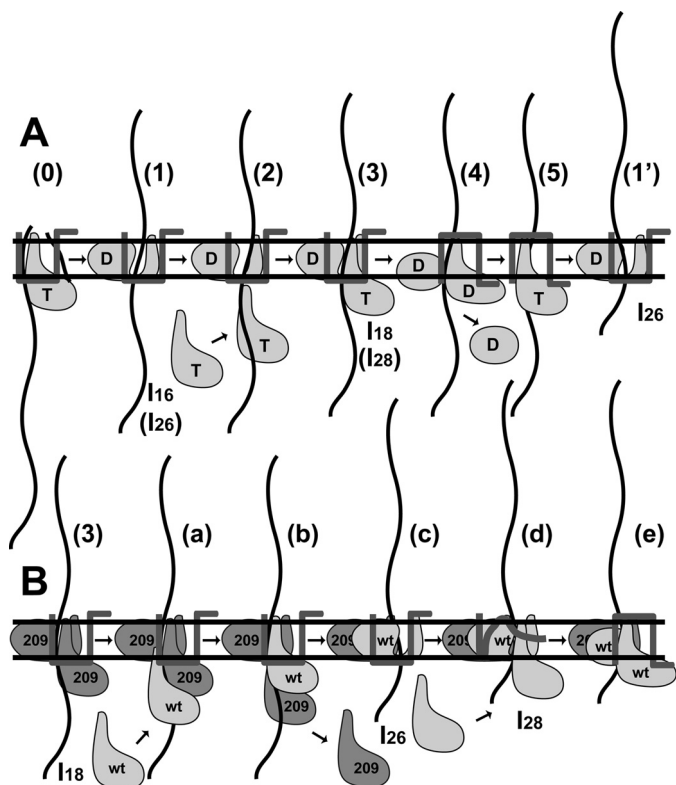


**FIGURE 6. Working model for proOmpA translocation.** A, WT SecA, SecG with its topology, and (pro)OmpA (waved line) are shown. T and D represent ATP and ADP, respectively. At step 0, cleavage of the signal sequence is shown. The extent of translocation (steps 1–5 and 1') is reflected by intermediate species (I<sub>16</sub>, I<sub>18</sub>, I<sub>26</sub>, and I<sub>28</sub>). B, model for the reaction involving D209N SecA. The mutant and wild-type SecA are indicated as 209 and WT. For details, see "Discussion."

type SecA. We cannot completely exclude the possibility that SecA associated with SecYEG protected SecG from the proteinase K digestion because both types of SecA should associate with the translocon under the conditions. However, either the central or C-terminal region of SecG was clearly digested under the other conditions. From these observations, it is likely that SecG inversion occurs when one SecA cycle is finished and the next cycle begins. This idea is consistent with the observation that the addition of AMP-PNP at the beginning of the translocation did not cause SecG inversion (13). As demonstrated previously (15, 45, 46), the SecA cycle is tightly coupled with the SecG function. Thus, D209N SecA was deinserted and replaced with newly added SecA if SecG was missing.

On the basis of our results and the observations so far reported together, the molecular mechanism underlying proOmpA translocation is illustrated in Fig. 6, focusing on the relationship between SecA and SecG. The signal peptide is cleaved on the periplasmic face of a membrane upon ATP binding to SecA, causing translocation by ~3 kDa (20) (Fig. 6A, step 0). With ATP hydrolysis, translocation proceeds, giving I<sub>16</sub> (20) (Fig. 6A, step 1). Because AMP-PNP addition to I<sub>16</sub> yields I<sub>18</sub>, a new SecA can function similar to initiation of translocation (20) (Fig. 6A, steps 2 and 3). Because D209N SecA itself can generate I<sub>18</sub> (Fig. 3A), and AMP-PNP cannot generate I<sub>16</sub>/I<sub>18</sub> (20), it is likely that ATP hydrolysis is necessary for the generation of I<sub>16</sub>. To move onto the next step, SecA that has been used to gener-

ate I<sub>16</sub> must be dislocated from translocon (steps 3 to 5). D209N SecA is unable to move onto these steps (Fig. 3A) and the mutant can fix the inverted topology of SecG (Fig. 2B). Therefore, ATP hydrolysis and SecG inversion should be necessary for such dislocation of SecA. In these steps, structure changes in SecA should be induced so that SecA is released from translocating proOmpA and thereby from translocon to be dislocated (step 4). It has been demonstrated that membrane-inserted SecA is transformed into a deinsertion-competent structure by ATP hydrolysis or PMF (39). After these steps with SecA dislocation, ADP should be exchanged with ATP (step 5) to allow the next steps, giving a subsequent intermediate (19, 20) (step 1'). After I<sub>26</sub> is formed, it will be fully translocated via I<sub>28</sub> into mature OmpA (34 kDa) (Fig. 3A), following steps similar to steps 2~5 and step 1'. Step 5 is similar to step 0 except that SecG is inverted in step 5. When an excess amount of AMP-PNP was added during translocation, it is likely that ATP is replaced with AMP-PNP in this step, resulting in the fixation of the inverted SecG. To recover the original topology of SecG, translocation of the C-terminal region of ~4 kDa is necessary, which also requires ATP hydrolysis (13). Next to I<sub>18</sub> is I<sub>26</sub>, the difference being ~8 kDa, which is shorter than the translocation comprising processing to I<sub>16</sub> (~13 kDa). Therefore, we speculate that when I<sub>26</sub> is formed, recovery of the SecG topology occurs simultaneously, giving a similar level of translocation. When the ATP concentration is low in the reaction, the ADP-ATP exchange should be rate-limiting. In our model, the cytosolic SecA and SecA in step 4 are candidates corresponding to steps 1 and 4, respectively. These facts explain why half of SecG was inverted when the ATP concentration was low (Fig. 2D). On the other hand, when D209N SecA was used, the reaction proceeded until step 3, giving I<sub>18</sub> (Fig. 3A). The addition of WT SecA at this step caused the generation of I<sub>28</sub> and mature OmpA with the transient appearance of I<sub>26</sub> (Fig. 3A) (Fig. 6B, steps a–e). Because WT SecA can be inserted into D209N SecA/proOmpA-loaded IMV (Fig. 3C), a part of membrane-associated D209N SecA should be dislocated and replaced by WT SecA (steps a and b). After this replacement, it is feasible that WT SecA translocates proOmpA, giving I<sub>26</sub> (Fig. 3A) (step c). This translocation is similar to one from step 5 to step 1'. However, membrane-associated mutant SecA cannot be replaced, as revealed by a protease protection assay involving radiolabeled SecA (Fig. 5). Because the conversion of I<sub>26</sub> into I<sub>28</sub> is achieved through ATP binding (19, 20), cytosolic SecA with ATP, irrespective of whether it is WT SecA or mutant SecA, should drive this translocation (step d). When D209N SecA is used in this case, the reaction should finish at this step with the accumulation of an intermediate topology of SecG (Fig. 2C). On the other hand, if WT SecA is used here, a structure change similar to that in step 4 can be caused, giving completely inverted SecG (Fig. 2C) (step e), followed by further translocation into mature OmpA (Fig. 3A). These facts explain why the same amounts of I<sub>28</sub> and mature OmpA were observed when the same amounts of WT SecA and D209N SecA were present (Fig. 3B). It might be possible that a new translocation begins after WT SecA completed translocation because the amount of I<sub>18</sub> formed by D209N SecA only was smaller than that of the sum of mature OmpA and intermediates in the presence of



both types of SecA (Fig. 3B). Nonetheless, after the I<sub>28</sub> formation, the D209N SecA-translocon complex becomes a dead-end one with which the next translocation cycle should not be allowed, explaining why D209N SecA shows a dominant-negative effect.

Using a proOmpA derivative carrying a mutation in signal peptide, translocation intermediates of 5 kDa, 10 kDa, and 21 kDa, in addition to I<sub>16</sub> and I<sub>26</sub>, have been identified under the low ATP conditions (21). Because the levels of the 10-kDa and 21-kDa ones were lower than others, these might be another series of translocation because of the mutation in signal peptide. In the case of the intermediate of 5 kDa, which we could not analyze under our gel conditions, it might be arisen by the result of the insertion of cytosolic SecA immediately after processing. Therefore, it is possible that I<sub>16</sub> was generated from the 5-kDa intermediate. Although it is not clear whether or not the additional intermediates were caused by the signal mutation, their appearance is compatible with our model because the interval between the 10-kDa and 21-kDa ones is ~10 kDa.

Our results indicate that SecA undergoes at least two different kinds of ATP hydrolysis. One is directly utilized in preprotein translocation and the other is used to cause SecA to move into the next SecA cycle. SecA possesses two NBDs (3). D209N SecA and R509K SecA are mutants to NBDs 1 and 2, and in these mutants high and low binding affinity with ADP is impaired, respectively, suggesting that SecA binds two ATP molecules (26). On the other hand, it has also been suggested that one ATP molecule is sandwiched by both NBDs (1, 3). Considering the appearance of translocation intermediates and the ability to fix the inverted topology of SecG, the roles of NBDs 1 and 2 are completely different, as demonstrated previously (23). Indeed, the inhibitory effects of two mutants on the translocation ATPase activity were quite different (Fig. 1E). Because the "insertion-deinsertion cycle" of R509K SecA seems normal (23), the inhibition by this mutant might be an indirect effect.

Several lines of evidence have demonstrated that SecA is inserted deep into a membrane (8, 9, 22). SecA can be digested or labeled from the periplasmic side, suggesting that SecA penetrates membranes (8). Not only the 30-kDa fragment (C terminus) but also the 65-kDa one (N terminus) of SecA, which is protected by membranes from proteinase K digestion, are detected coupled with proOmpA translocation (47). These findings strongly support SecA insertion, although the 30-kDa fragment can be partially detected in the presence of detergent-solubilized SecYEG (48). A fraction of membrane-associated SecA is also resistant to alkaline extraction of IMV (5), indicating that these fractions are membrane-integrated. On the other hand, crystals of SecYEG (25, 49) and the SecA-SecYEG complex (24) revealed that the SecA insertion model is not favorable because the pores of the translocon seem too small for SecA insertion, and the position of SecA on SecYEG is far away from the membrane surface. However, both SecA and SecYEG undergo several kinds of structural changes. Therefore, the structures during translocation, such as that of SecYEG with inverted SecG or translocating preproteins, have not yet been clarified. Moreover, although SecYEG overproduction significantly enhances the translocation activity, the specific activity

per SecYEG is quite low compared with in IMV prepared from the wild-type strain (45, 50, 51). Furthermore, SecG inversion could not be detected under the SecYEG-overproducing conditions (17, 18), strongly suggesting the presence of unknown factor(s) involved in translocation. Even if SecA might not be inserted deep into membranes, our results demonstrate that multiple SecA molecules function on a single translocon.

PMF is utilized for translocation as another energy source, although PMF may not be essential (29, 52). At the late stage of translocation (19, 20) or for preproteins with partially folded structures (31, 44), only PMF can drive translocation without ATP hydrolysis. According to our results, even I<sub>28</sub>, which was accumulated by mutant SecA, was translocated into mature OmpA by PMF (Fig. 4). It is reported that even D209N SecA inserted into membrane was deinserted by PMF (39), which should allow the translocation of I<sub>28</sub>. Alternatively, SecDF might be involved in such translocation, as reported recently (53). In any case, the proton movement is important for the PMF-dependent translocation (39, 52), unlike the electrophoretic movement caused by the membrane potential observed on membrane insertion of a subset of Sec-independent membrane proteins (54). These findings strongly suggest that the translocon undergoes a dynamic structure change caused by PMF. The observation that precursors artificially attached to a large domain can be translocated in the presence of PMF (41, 42, 55) is also consistent with this idea. As a high concentration of soluble SecA complements the lack of PMF (38), it is likely that cytosolic SecA induces a similar structure change in the translocon.

---

*Acknowledgments*—We thank Prof. D. Oliver (Wesleyan University) for the gift of the plasmids. We also thank Dr. S. Tomioka (University of Tokyo) for help with protein sequencing.

---

## REFERENCES

1. Kusters, I., and Driessen, A. J. (2011) *Cell Mol. Life Sci.* **68**, 2053–2066
2. du Plessis, D. J., Nouwen, N., and Driessen, A. J. (2011) *Biochim. Biophys. Acta* **1808**, 851–865
3. Sardis, M. F., and Economou, A. (2010) *Mol. Microbiol.* **76**, 1070–1081
4. Rapoport, T. A. (2007) *Nature* **450**, 663–669
5. Cabelli, R. J., Dolan, K. M., Qian, L. P., and Oliver, D. B. (1991) *J. Biol. Chem.* **266**, 24420–24427
6. Lill, R., Dowhan, W., and Wickner, W. (1990) *Cell* **60**, 271–280
7. de Vrije, T., de Swart, R. L., Dowhan, W., Tommassen, J., and de Kruijff, B. (1988) *Nature* **334**, 173–175
8. Kim, Y. J., Rajapandi, T., and Oliver, D. (1994) *Cell* **78**, 845–853
9. Watanabe, M., and Blobel, G. (1993) *Proc. Natl. Acad. Sci. U.S.A.* **90**, 9011–9015
10. Akita, M., Shinkai, A., Matsuyama, S., and Mizushima, S. (1991) *Biochem. Biophys. Res. Commun.* **174**, 211–216
11. Nishiyama, K., Mizushima, S., and Tokuda, H. (1993) *EMBO J.* **12**, 3409–3415
12. Nishiyama, K., Hanada, M., and Tokuda, H. (1994) *EMBO J.* **13**, 3272–3277
13. Nishiyama, K., Suzuki, T., and Tokuda, H. (1996) *Cell* **85**, 71–81
14. Nagamori, S., Nishiyama, K., and Tokuda, H. (2000) *J. Biochem.* **128**, 129–137
15. Suzuki, H., Nishiyama, K., and Tokuda, H. (1998) *Mol. Microbiol.* **29**, 331–341
16. Nagamori, S., Nishiyama, K., and Tokuda, H. (2002) *J. Biochem.* **132**, 629–634

## SecA-SecE Cycle in Preprotein Translocation

17. Sugai, R., Takemae, K., Tokuda, H., and Nishiyama, K. (2007) *J. Biol. Chem.* **282**, 29540–29548
18. van der Sluis, E. O., van der Vries, E., Berrelkamp, G., Nouwen, N., and Driessen, A. J. (2006) *J. Bacteriol.* **188**, 1188–1190
19. Tani, K., Shiozuka, K., Tokuda, H., and Mizushima, S. (1989) *J. Biol. Chem.* **264**, 18582–18588
20. Schiebel, E., Driessen, A. J., Hartl, F. U., and Wickner, W. (1991) *Cell* **64**, 927–939
21. van der Wolk, J. P., de Wit, J. G., and Driessen, A. J. (1997) *EMBO J.* **16**, 7297–7304
22. Economou, A., and Wickner, W. (1994) *Cell* **78**, 835–843
23. Economou, A., Pogliano, J. A., Beckwith, J., Oliver, D. B., and Wickner, W. (1995) *Cell* **83**, 1171–1181
24. Zimmer, J., Nam, Y., and Rapoport, T. A. (2008) *Nature* **455**, 936–943
25. Van den Berg, B., Clemons, W. M., Jr., Collinson, L., Modis, Y., Hartmann, E., Harrison, S. C., and Rapoport, T. A. (2004) *Nature* **427**, 36–44
26. Mitchell, C., and Oliver, D. (1993) *Mol. Microbiol.* **10**, 483–497
27. Yamane, K., Ichihara, S., and Mizushima, S. (1987) *J. Biol. Chem.* **262**, 2358–2362
28. Hanada, M., Nishiyama, K. I., Mizushima, S., and Tokuda, H. (1994) *J. Biol. Chem.* **269**, 23625–23631
29. Yamada, H., Tokuda, H., and Mizushima, S. (1989) *J. Biol. Chem.* **264**, 1723–1728
30. Akita, M., Sasaki, S., Matsuyama, S., and Mizushima, S. (1990) *J. Biol. Chem.* **265**, 8164–8169
31. Tani, K., Tokuda, H., and Mizushima, S. (1990) *J. Biol. Chem.* **265**, 17341–17347
32. Shinkai, A., Akita, M., Matsuyama, S., and Mizushima, S. (1990) *Biochem. Biophys. Res. Commun.* **172**, 1217–1223
33. Laemmli, U. K. (1970) *Nature* **227**, 680–685
34. Hussain, M., Ichihara, S., and Mizushima, S. (1980) *J. Biol. Chem.* **255**, 3707–3712
35. Nishiyama, K., Mizushima, S., and Tokuda, H. (1992) *J. Biol. Chem.* **267**, 7170–7176
36. Tokuda, H., Yamanaka, M., and Mizushima, S. (1993) *Biochem. Biophys. Res. Commun.* **195**, 1415–1421
37. Lowry, O. H., Rosebrough, N. J., Farr, A. L., and Randall, R. J. (1951) *J. Biol. Chem.* **193**, 265–275
38. Yamada, H., Matsuyama, S., Tokuda, H., and Mizushima, S. (1989) *J. Biol. Chem.* **264**, 18577–18581
39. Nishiyama, K., Fukuda, A., Morita, K., and Tokuda, H. (1999) *EMBO J.* **18**, 1049–1058
40. Matsuyama, S., Kimura, E., and Mizushima, S. (1990) *J. Biol. Chem.* **265**, 8760–8765
41. Tani, K., and Mizushima, S. (1991) *FEBS Lett.* **285**, 127–131
42. Kato, M., and Mizushima, S. (1993) *J. Biol. Chem.* **268**, 3586–3593
43. Joly, J. C., and Wickner, W. (1993) *EMBO J.* **12**, 255–263
44. Uchida, K., Mori, H., and Mizushima, S. (1995) *J. Biol. Chem.* **270**, 30862–30868
45. Duong, F., and Wickner, W. (1997) *EMBO J.* **16**, 2756–2768
46. Matsumoto, G., Yoshihisa, T., and Ito, K. (1997) *EMBO J.* **16**, 6384–6393
47. Eichler, J., and Wickner, W. (1997) *Proc. Natl. Acad. Sci. U.S.A.* **94**, 5574–5581
48. van der Does, C., Manting, E. H., Kaufmann, A., Lutz, M., and Driessen, A. J. (1998) *Biochemistry* **37**, 201–210
49. Tsukazaki, T., Mori, H., Fukai, S., Ishitani, R., Mori, T., Dohmae, N., Perederina, A., Sugita, Y., Vassilyev, D. G., Ito, K., and Nureki, O. (2008) *Nature* **455**, 988–991
50. Douville, K., Price, A., Eichler, J., Economou, A., and Wickner, W. (1995) *J. Biol. Chem.* **270**, 20106–20111
51. van der Does, C., den Blaauwen, T., de Wit, J. G., Manting, E. H., Groot, N. A., Fekkes, P., and Driessen, A. J. (1996) *Mol. Microbiol.* **22**, 619–629
52. Shiozuka, K., Tani, K., Mizushima, S., and Tokuda, H. (1990) *J. Biol. Chem.* **265**, 18843–18847
53. Tsukazaki, T., Mori, H., Echizen, Y., Ishitani, R., Fukai, S., Tanaka, T., Perederina, A., Vassilyev, D. G., Kohno, T., Maturana, A. D., Ito, K., and Nureki, O. (2011) *Nature* **474**, 235–238
54. Kuhn, A. (1995) *FEMS Microbiol. Rev.* **17**, 185–190
55. Bonardi, F., Halza, E., Walko, M., Du Plessis, F., Nouwen, N., Feringa, B. L., and Driessen, A. J. (2011) *Proc. Natl. Acad. Sci. U.S.A.* **108**, 7775–7780